Isomeric polyimides for gas separation membranes

Jingling Yan(阎敬灵)[a, b], Xiaofan Hu [a], and Zhen Wang（王震） [a]*

[a] Polymer Composites Engineering Laboratory, Changchun Institute of Applied Chemistry, Chinese Academy of Science, Changchun 130022, China.

b Division of Specialty Fibers, Ningbo Institute of Materials Technology and Engineering, Chinese Academy of Science, Ningbo 315201, China

** Corresponding author: Email: jyan@nimte.ac.cn.*

1. Introduction

Recently, many research efforts have been devoted to the development of polymeric gas separation membranes, which possess several inherent advantages over the incumbent technologies, including high efficiency, low waste generation, and high cost-effectiveness. The majority of glassy polymers show high gas selectivity but low gas permeability, which prevents their widespread applications. Polymers of intrinsic microporosity (PIMs), firstly reported by McKeown and Budd in 2004, feature rigid and kinked structures, which could restrict efficient chain packing and chain motion. The unique architectures of PIMs result in the formation of micropores with a width of ＜2 nm. The gas sieving effects of micropores lead to high permeabilities and gas pair selectivities[1-6]. The Robeson upper-bound plot, based on the data of reported polymers, is a vital empirical criterion to judge the gas separation performance of polymeric membranes[7-9].

Polyimides have been explored as gas separation membranes owing to their high selectivity, and excellent thermal and mechanical properties. However, except 4,4'-(hexafluoroisopropylidene)diphthalic anhydride (6FDA), most commercial bridged dianhydrides have linear configurations originated from their 4,4'-connections, which couldn't effectively frustrate chain packing. On the contrary, isomeric dianhydrides with 3,4'- or 3,3'-linked geometry are expected to produce polyimides with bent and steric hindered architectures, which could facilitate fast gas permeation. In this work, we present the synthesis and characterization of TB-containing PIM-PIs from isomeric biphenyltetracarboxylic dianhydrides (BPDA) and isomeric oxydiphthalic anhydrides (ODPA), and their gas separation performance were comparatively investigated according to their surface area, inter-chain distance, and gas separation performance. The results revealed that polymers derived from 3,3'-biphenyltetracarboxylic dianhydride (3,3'-BPDA) showed improved gas separation performance compared with those from 6FDA for certain diamines.

2. Results and discussion

TB-containing PIM-PIs from isomeric ODPAs, isomeric BPDAs, and 6FDA were synthesized as depicted in Scheme 1. The specific BET surface areas of the isomeric polyimides were in the range of 16-416 $m^2 g^{-1}$. In general, the BET surface areas of PIMs were dictated by the rigidity and rotational barrier of the polymer backbones. For PIM-PIs based on TBDA1, their BET surface areas followed the order of 3,3'-BPDA > 6FDA > 4,4'-BPDA > 3,3'-ODPA > 3,4'-ODPA > 4,4'-ODPA > 3,4'-BPDA. Polyimides based on isomeric ODPAs possessed relatively lower BET surface areas compared with those based on isomeric BPDAs, which could be attributed to the existence of flexible ether linkages**.** In contrast, 3,3'-BPDA- and 6FDA- derived polyimides exhibited high BET surface areas, which was related with their non-coplanar, rotation-restricted structures. The dihedral angels between two phenyl rings for 3,3'-BPDA and 6FDA are 64.0° and 65.6°, respectively, which gave rise to the loosely

packed polymer chains. In spite of coplanar configuration and lower rotational barrier, 4,4'-BPDA-based polymers also showed high BET surface areas because of their high chain rigidity, especially for 4,4'-BPDA-TBDA2. However, the 3,4'-BPDA-based polymers showed relative lower BET surface areas, which could be explained by their asymmetric structures that tends to the form more coiled chains. A sharp rise at low pressure region (P/P_0 = 0.2-0.3) was observed in the nitrogen adsorption and desorption isotherms of 3,4'-BPDA-TBDA2, indicating the presence of mesopores. The pore size distributions (PSD) obtained from CO_2 isotherms using HK method centered at around 0.7 nm, suggesting the presence of micropores. Furthermore, total pore volumes, FFV, and *d*-spacing showed similar tendency to that of BET surface areas.

The gas separation results for PIM-PIs derived from isomeric BPDAs and ODPAs were displayed in Table 2 and Figure 2. The pure gas permeability of isomeric polyimides were in the order of 3,3'-BPDA-TBDA2>3,3'-BPDA-TBDA1>6FDA-TBDA2>4,4'-BPDA-TBDA2>3,4'-BPDA-TBDA2> 6FDA-TBDA1>4,4'-BPDA-TBDA1>3,3'-ODPA-TBDA1>3,4'-ODPA-TBDA1>4,4'-ODPA-TBDA1> 3,4'-BPDA-TBDA1. 3,3'-BPDA-TBDA2 exhibited the highest gas permeabilities among all the polymers, 1.7-1.8 times larger than those of 6FDA-TBDA2. Besides high permeabilities 3,3'-BPDA-TBDA2 also exhibited an ideal selectivity of 4.20 for O_2/N_2, 20.2 for CO_2/N_2, 32.5 for CO_2/CH_4.

3. Conclusions

In this work, PIM-PIs were synthesized using isomeric BPDAs and ODPAs as the monomers, and their physical properties and gas separation performance were comprehensively investigated. Due to their rigid but non-coplanar architectures, polyimides derived from 3,3'-BPDA showed highest BET surface areas, FFV and interchain distances among isomeric polyimides. Consequently, 3,3'-BPDA-based polyimides exhibited improved gas separation performance in comparison with those based on 6FDA, evidenced by Robeson's upper bound.

Acknowledgement

The work was financially supported by the National Natural Science Foundation of China (No. 51473157).

References

[1]. Lee, M.; Bezzu, C. G.; Carta, M.; Bernardo, P.; Clarizia, G.; Jansen, J. C.; McKeown, N. B. *Macromolecules* **2016,** *49* (11), 4147-4154.

[2]. Ghanem, B. S.; McKeown, N. B.; Budd, P. M.; Fritsch, D. Macromolecules 2008, 41 (5), 1640-1646.

[3]. Ghanem, B. S.; McKeown, N. B.; Budd, P. M.; Al-Harbi, N. M.; Fritsch, D.; Heinrich, K.; Starannikova, L.; Tokarev, A.; Yampolskii, Y. Macromolecules 2009, 42 (20), 7881-7888.

[4]. Budd, P. M.; Ghanem, B. S.; Makhseed, S.; McKeown, N. B.; Msayib, K. J.; Tattershall, C. E. Chemical Communications 2004, (2), 230.

[5]. Wang, S.; Li, X.; Wu, H.; Tian, Z.; Xin, Q.; He, G.; Peng, D.; Chen, S.; Yin, Y.; Jiang, Z.; Guiver, M. D. Energy & Environmental Science 2016, 9 (6), 1863-1890.

[6]. Low, Z.-X.; Budd, P. M.; McKeown, N. B.; Patterson, D. A. Chemical Reviews 2018, 118 (12), 5871-5911.

[7]. Robeson, L. M. Journal of Membrane Science 1991, 62 (2), 165-185.

[8]. Robeson, L. M. Journal of Membrane Science 2008, 320 (1), 390-400.

[9]. Swaidan, R.; Ghanem, B.; Pinnau, I. ACS Macro Letters 2015, 4 (9), 947-951.

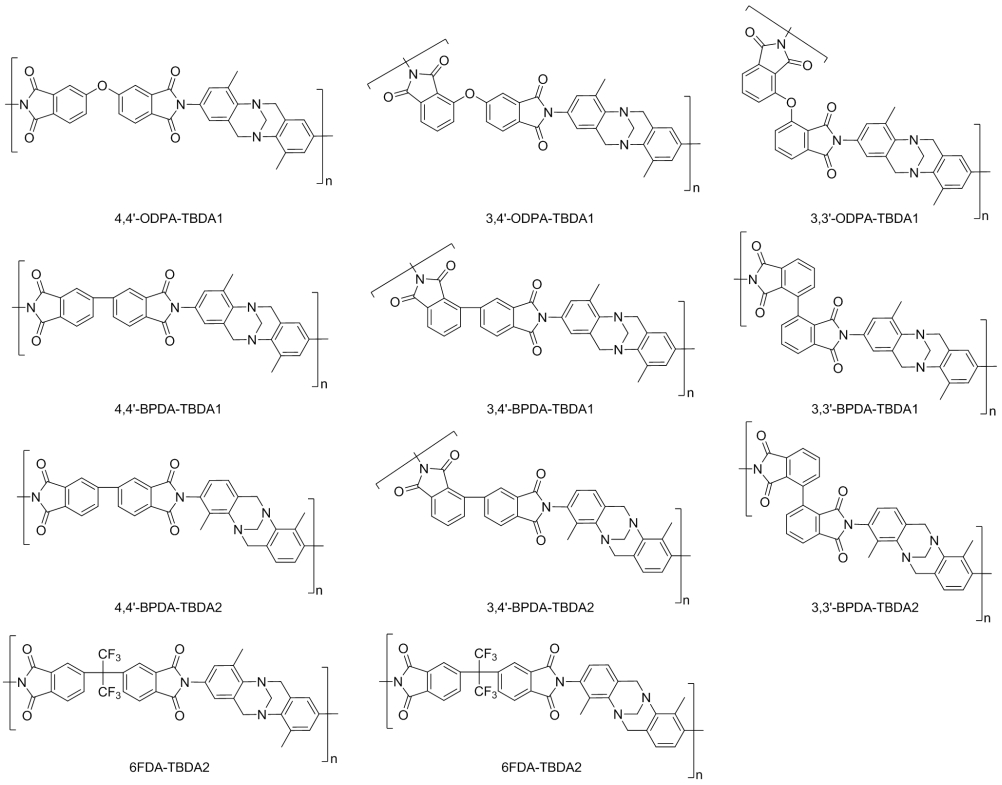

Scheme 1. Synthesis of isomeric polyimides.

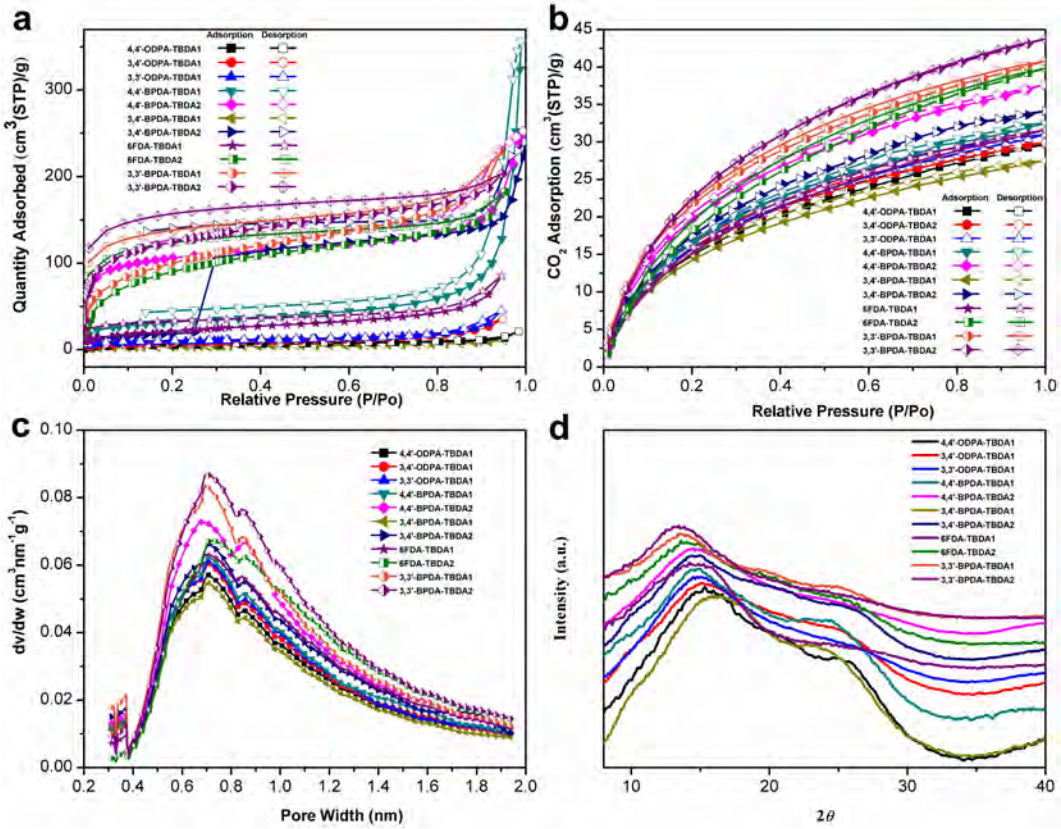

Figure 1. (a) Nitrogen adsorption/desorption isotherms of isomeric polyimides measured at 77 K. (b) CO_2 adsorption and desorption isotherms at 273 K for isomeric polyimides. (c) Pore width distributions estimated from CO_2 sorption isotherms using the Horváth-Kawazoe (HK) method assuming carbon slit-pore geometry. (d)

WAXD analyses of isomeric polyimides membranes.

Table 1. Physical properties of isomeric polyimides

Polyimides	S_{BET}, $m^2\ g^{-1}$	V_{Tot},[a] $cm^3\ g^{-1}$	D_{Pore}, [b] nm	CO_2 uptake[c] (cm^3/g)	*d*-spacing (nm)	ρ (g/cm^3)	FFV
4,4'-ODPA-TBDA	26	0.111	0.70/0	29.7	0.578	1.289	0.123
3,4'-ODPA-TBDA	27	0.088	0.70/0	29.9	0.590	1.286	0.125
3,3'-ODPA-TBDA	32	0.114	0.71/0	31.0	0.601	1.278	0.130
4,4'-BPDA-TBDA	108	0.136	0.71/0	32.5	0.604	1.251	0.139
4,4'-BPDA-TBDA	338	0.333	0.68/0	37.6	0.614	1.230	0.153
3,4'-BPDA-TBDA	16	0.015	0.70/0	27.5	0.557	1.293	0.110
3,4'-BPDA-TBDA	164	0.143	0.71/0	34.2	0.608	1.235	0.150
6FDA-TBDA1	76	0.132	0.70/0	31.6	0.607	1.359	0.150
6FDA-TBDA2	314	0.282	0.72/0	39.8	0.621	1.349	0.157
3,3'-BPDA-TBDA	351	0.315	0.69/0	40.8	0.642	1.219	0.161
3,3'-BPDA-TBDA	416	0.353	0.70/0	43.8	0.665	1.215	0.164

[a] Total pore volume at $P/P_0 = 0.95$.

[b] Determined by maxima of the PSD using HK model.

[c] CO_2 uptake determined volumetrically at 1.00 bar and 273.15 K.

[d] Measured by WAXD.

Table 2. Gas Permeability (P) and Ideal Selectivity (α) of isomeric polyimides[a]

Polyimides	Permeability					selectivity			
	He	CO_2	O_2	N_2	CH_4	He/CH_4	O_2/N_2	CO_2/N_2	CO_2/CH_4
4,4'-ODPA-TBDA1	13.2	11.5	1.8	0.35	0.27	49	5.0	33	43
3,4'-ODPA-TBDA1	15.6	12.4	2.0	0.39	0.28	56	5.2	32	44
3,3'-ODPA-TBDA1	18.1	13.3	2.2	0.43	0.32	56	5.1	31	42
4,4'-BPDA-TBDA1	35.2	29.3	7.2	1.6	0.98	36	4.6	18	30
4,4'-BPDA-TBDA2	192	173	35	6.6	4.2	45	5.2	26	41
3,4'-BPDA-TBDA1	10.6	8.6	1.7	0.31	0.19	56	5.5	28	45
3,4'-BPDA-TBDA2	177	134	26.1	6.0	4.5	39	4.3	22	30
6FDA-TBDA1	172	120	24.5	5.1	3.3	52	4.8	24	36
6FDA-TBDA2	198	194	39.2	9.1	5.7	35	4.3	21	34
3,3'-BPDA-TBDA1	264	252	52.4	12.4	7.5	35	4.2	20	34
3,3'-BPDA-TBDA2	349	338	70.2	16.7	10.4	34	4.2	20	32

[a] 1 barrer = 10^{-10} [cm^3(STP) cm]/(cm^2s cm Hg).

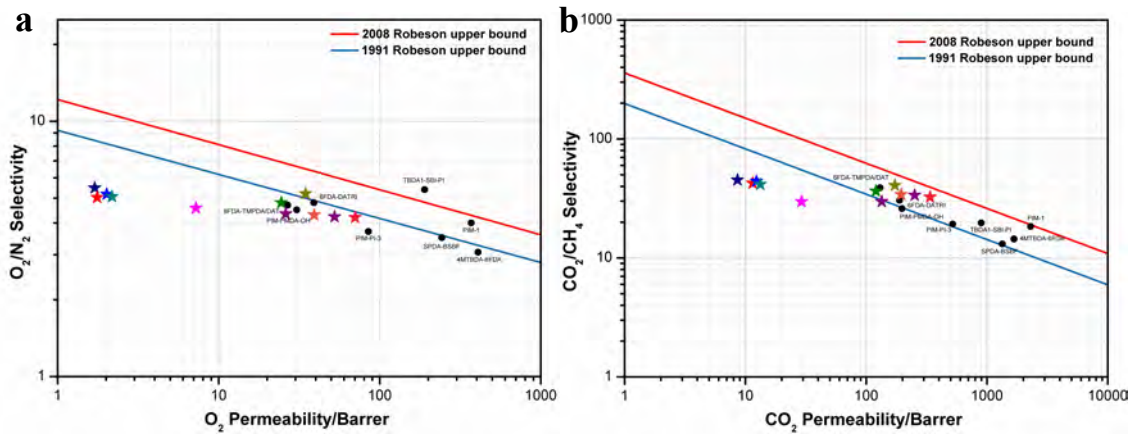

Figure 2. Relationship between gas permeability (P) and gas pair selectivity (α) with Robeson upper bound (red ★: 4,4'-ODPA-TBDA1; blue ★: 3,4'-ODPA-TBDA1; dark cyan ★: 3,3'-ODPA-TBDA1; magenta ★: 4,4'-BPDA-TBDA1; dark yellow ★: 4,4'-BPDA-TBDA2; navy ★: 3,4'-BPDA-TBDA1; purple ★: 3,4'-BPDA-TBDA2; olive ★: 6FDA-TBDA1; orange ★: 6FDA-TBDA2; violet ★: 3,3'-BPDA-TBDA1; pink ★: 3,3'-BPDA-TBDA2): (a) for O_2/N_2 and (b) for CO_2/CH_4. Other data points stand for representative polymers with high permeability reported since the upper bounds were updated in 2008.